Pinty, B., Verstraete, M.M. and Dickinson, R.E., 1989. A physical model for predicting bidirectional reflectances over bare soil. Remote Sensing Environ., 27: 273–288.
Pinty, B., Verstraete, M.M. and Dickinson, R.E., 1990. A physical model of the bidirectional reflectance of vegetation canopies. 2. Inversion and validation. J. Geophys. Res., 95: 11 767–11 775.
Privette, J.L., Myneni, R.B., Tucker, C.J. and Emery, W.J., 1994. Invertibility of a 1-D discrete ordinates canopy reflectance model. Remote Sensing Environ., 48: 89–105.
Rahman, H., Pinty, B. and Versraete, M.M., 1993. Coupled surface atmosphere reflectance (CSAR) model. Part 2: semiempirical surface model usable with NOAA AVHRR data. J. Geophys. Res., 98(D11): 20791–20801.
Ranson, K.J., Irons, J.R. and Daughtry, C.S.T., 1991. Surface albedo from bidirectional reflectance. Remote Sensing Environ., 35: 201–211.
Ross, J., 1981. The Radiation Regime and Architecture of Plant Stands. Junk, The Hague, 391 pp.
Ross, J.K. and Marshak, A.L., 1988. Calculation of canopy directional reflectance using the Monte Carlo Method. Remote Sensing Environ., 24: 213–225.
Roujean, J.L., Leroy, M. and Deschamps, P.Y., 1992. A bidirectional reflectance model of the Earth's surface for the correction of remote sensing data. J. Geophys. Res., 97(D18): 20455–20468.
Running, S.W., Justice, C.O., Salomonson, V., Hall, D., Barker, J., Kaufmann, Y.J., Strahler, A.H., Huete, A.R., Muller, J.-P., Vanderbilt, V., Wan, Z.M., Teillet, P. and Carneggie, D., 1994. Terrestrial remote sensing science and algorithms planned for EOS/MODIS. Int. J. Remote Sensing, 15(17): 3587–3620.
Salomonson, V.V., Barnse, W.L., Maymon, P.W., Montgomery, H.E. and Ostrow, H., 1989. MODIS: advanced facility instrument for studies of the earth as a system. IEEE Trans. Geosci. Remote Sensing, GE-27: 145–153.
Strahler, A.H., Wanner, W., Zhu, Q. and Jin, X., 1995a. Bidirectional reflectance modeling of data from vegetation obtained in the Changchun solar simulation laboratory. In: T.I. Stein (Editor), Proceedings of the International Geoscience and Remote Sensing Society Symposium, July 1995, Firenze, Italy, IEEE, Pitscataway, NJ.
Strahler, A.H., Wanner, W., Li, X., Muller, J.P., Barnsley, M.J. and Lewis, P., 1995b. MODIS BRDF/Albedo product: algorithm technical basis document, Version 3.1, NASA EOS MODIS, NASA, Washington, DC.
Vermote, E., Tanré, D., Deuzé, J.L., Herman, M. and Morcette, J.J., 1994. Second Simulation of the Satellite Signal in the Solar Spectrum (6S User Guide) (unpublished).
Verstraete, M.M., Pinty, B. and Dickinson, R.E., 1990. A physical model of the bidirectional reflectance of vegetation canopies. 1. Theory. J. Geophys. Res., 95: 11 755–11 765.
Wallace, J.S., Brouwer, J., Allen, S.J., Banthorpe, D., Blyth, E.M., Blyth, K., Bromley, J., Buerkert, A.C., Cantwell, M., Cooper, J.D., Cropley, F.D., Cuff, A.D., Dolman, A.J., Dugdale, G., Gash, J.H.C., Gaze, S.R., Harding, R.J., Harrison, R.G., Holwell, C.J., Jarvis, P.G., Levy, P.E., Lloyd, C.R., Malhi, Y.S., Massheder, J.M., Moncrieff, J.B., Pearson, D., Settle, J.J., Sewell, I.J., Sivakumar, M.V.K., Sudlow, J.D., Taylor, C.M., Wilson, A.K., 1994. HAPEX-SAHEL Southern Super-Site Report: An Overview of the Site and the Experimental Programme During the Intensive Observation Period in 1992. Institute of Hydrology, Wallingford, 55 pp.
Walthall, C.L., Norman, J.M., Welles, J.M., Campbell, G. and Blad, B.L., 1985. Simple equation to approximate the bidirectional reflectance from vegetative canopies and bare soil surfaces. Appl. Opt., 24: 383–387.
Wanner, W., Li, X. and Strahler, A.H., 1995. On the derivation of kernels for kernel-driven models of bidirectional reflectance. J. Geophys. Res., 100: 21077–21089.
Wilson, M.F. and Henderson-Sellers, A., 1985. A global archive of land cover and soils data for use in GCMs. J. Climatol., 5: 119–143.

Fonds Documentaire IRD
010021618

ELSEVIER

Journal of Hydrology 188–189 (1997) 779–787

Journal of Hydrology

Determination of vegetation parameters through measured and simulated AVHRR data over SALT–HAPEX-Sahel site

V. Gond[a,*], F. Cabot[a], A. Chehbouni[b], J.-C. Meunier[a]

[a]*LERTS, 18 avenue E. Belin, 31055 Toulouse cedex, France*
[b]*ORSTOM, Hydrology Laboratory, Montpellier, France*

Abstract

Vegetation-related information is critical for modelling hydrological processes. Remotely sensed spectral data provide powerful means to characterize vegetation state. In this study, we investigate the opportunities of such data when an automatic classification is applied to time-series of remotely sensed data. The analysis is then conducted by interpreting the classification results in terms of surface physical parameters. The method consists in (1) selecting several control points in the HAPEX-Sahel square degree, during the rainy season of 1991 and 1992, and (2) comparing the temporal evolution of the albedo-based normalized difference vegetation index (NDVI) values and those deriving from the classification. The result shows that there is similarity between the behaviour of the 1991 and 1992 temporal profiles estimated at all control points.

1. Introduction

Vegetation has been identified as one of the most important surface parameters that influence water, energy and CO_2 cycles. The vegetation modifies the distribution of precipitation such as surface runoff and infiltration. Its amount also controls the partitioning of available energy at the surface into sensible and latent heat fluxes as well as respiration and photosynthetic processes. Consequently, changes in vegetation amount will lead in the long term to changes in the local and global climates, which in turn, as a feedback, will affect the vegetation growth. Thus, substantial information on vegetation canopies is needed to support the investigation of the effects of surface processes on climate processes in Sahelian region.

* Corresponding author.

0022-1694/97/$17.00 © 1997– Elsevier Science B.V. All rights reserved
PII S0022-1694(96)03170-8

Fonds Documentaire IRD
Cote : B* 21618 Ex : 1

Remote sensing is a powerful tool to characterize vegetation state and dynamics. Radiometric measurements, in the solar spectral domain, contain useful information about vegetation. Analysis of remotely sensed data has revealed the existence of real possibilities to estimate vegetation properties such as leaf area index (LAI), percentage of vegetation cover, interceptive photosynthetically active radiation (IPAR), and green biomass (Asrar et al., 1984). Such data, however, depend on atmospheric effects, background soil scattering, and, in particular, viewing and illumination geometry. The desire to use satellite potentialities represents a challenge for quantitative interpretations of these measurements.

The objective of the present study is to use remotely sensed data to characterize the spatial and temporal evolution of the surface for the HAPEX-Sahel square degree, during the rainy seasons of 1991 and 1992. An automatic classification is used to discriminate different vegetation type classes based on their temporal dynamics. Then, for some of the dominant classes within the square degree, control pixels are defined to verify the consistency of the classification. This selection is performed by comparing the temporal behaviour of the observed normalized difference vegetation index (NDVI) for a known pixel within a given class with the corresponding albedo-based NDVI, which is obtained by a least-squares fitting of surface reflectances from a bidirectional reflectance model and a numerical and iterative algorithm of minimization (quasi-Newton method). Finally, the results obtained by the classification are qualitatively compared with an actual surface map.

2. Material and method

Our study zone is in a typical sahelian zone, in the southwest of Niger. This study is within the framework of two international projects: the SALT (SAvanna on the Long Term) programme (Menaut and Podaire, 1990) and the HAPEX-Sahel experiment (Goutorbe et al., 1994). The objective of the SALT project is to understand the dynamics of the savanna over two transects in West Africa. A latitudinal transect crosses different savanna cover types, and a longitudinal one is located in the sahelian zone. In the present investigation, we use only one of the eight ground squares of the SALT experiment, which corresponds to the HAPEX-Sahel study site. In the east and south zone of the square degree, we located three well-documented sites, where the vegetation is typically fallow, millet and tiger bush (Fig. 1).

2.1. *AVHRR data*

AVHRR data over the square degree during a 2 year period (1991–1992) have been used in this study. The time-series extend through the rainy season, from the beginning of May to the end of October. Data preprocessing includes accurate calibration (Teillet and Holben, 1994) and atmospheric correction. Corrections of water vapour, ozone and dust content effects on surface reflectances in the visible (0.58–0.68 nm) and near-IR (0.72–1.10 nm) spectral bands are performed with a simplified model named SMAC

(Rahman and Dedieu, 1994). For each year, 160 windows corresponding to 102 km by 102 km, centred over the square degree, are extracted from the AVHRR scenes. A thermal IR-based method (INTUITIV: Loudjani et al., 1994) is applied to eliminate residual perturbations from atmospheric contaminations.

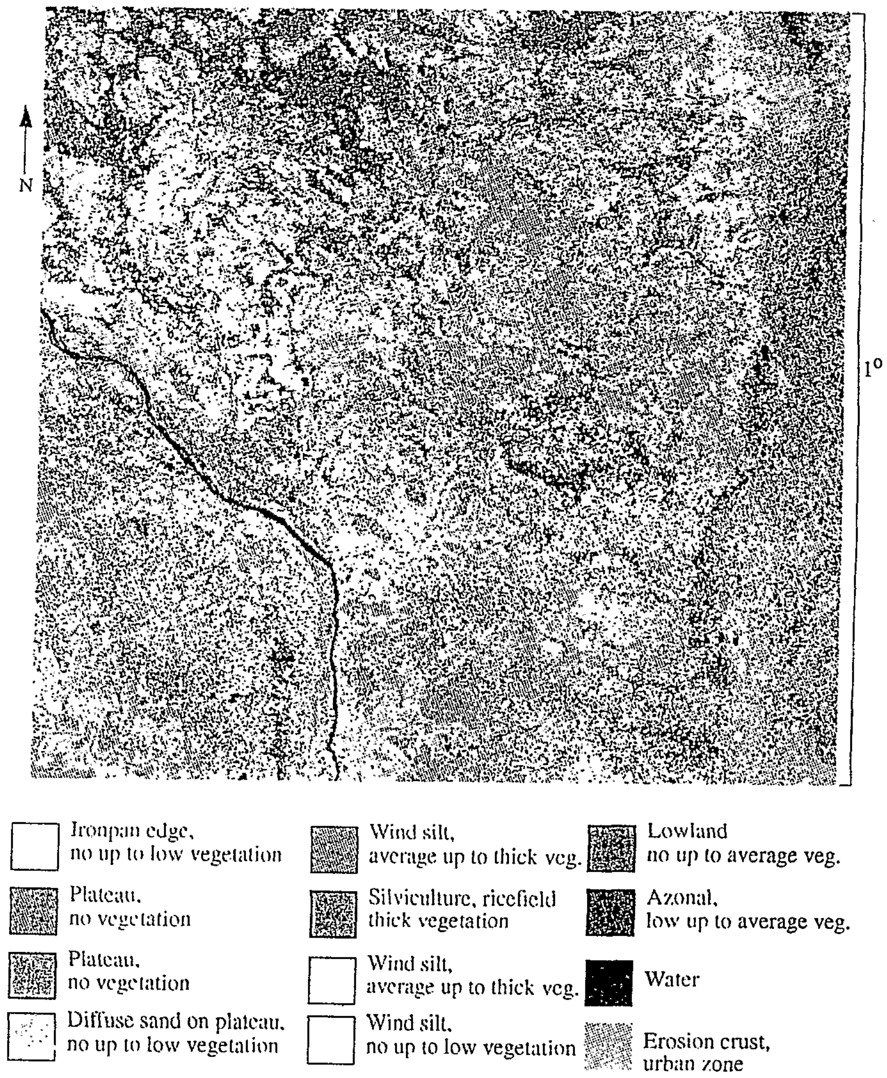

Fig. 1. Introduction to the map 'Etat de surface du sol, degré², Niamey, Niger' (Square degree surface order, Niamey, Niger) by Valentin et al. (1992).

2.2. *Automatic classification*

The general principle of the method is to look for clouds of points in the image, perhaps using only a sample of the pixels (Viovy, 1990). The method is recursive, and starts from a single class representing the whole vector space. It then splits this single initial cloud into two dichotomous clouds and converges towards the clouds of points (Fig. 2). It should be pointed out that the method works on each pixel individually and does not take into account spatial relationships between pixels.

An $(n+1)$-dimensional space $D = J \times C$ is defined, where $j \in J$ is the day number and C is the channel set used at a given wavelength (in our case, C corresponds to NDVI channel). In this space, $X(j, x_1, \ldots, x_n)$ represents the value of a pixel. Areas on the ground are represented by a cloud of points. Distinct clouds correspond to areas with different spectral identities at a given time. The principle of the automatic classification is to identify these clouds of points and to subdivide the space so that each class is made up of a single cloud. Each point is then allocated to the nearest class.

At each iteration, we suppose that each class is made up of two distinct clouds of points. We therefore seek an approximate centre for these two new classes, starting from the centre of the initial class and from its statistical properties. This strategy allows a new division of the vector space. Each point is then re-allocated to one of the new classes with respect to the newly estimated centres. Finally, we recalculate the real centre of each new class. A great advantage of the method is that its complexity is linearly related to the number of channels, which allows its use on long time-series and large numbers of channels.

2.3. *Bidirectional reflectance model*

Although it is not always desirable to have off-nadir viewing angle measurements from remote sensing platforms because of the bidirectional effects, as mentioned in the previous sections, sensors with off-nadir viewing angles provide more various information on vegetation. This is due primarily to vegetation structure. Tall vegetation species create larger shadows, but they also expose a larger portion of their vertical structure to the sensing systems when viewed from off-nadir directions. Consequently, the off-nadir viewing angle measurements can be used to study the vegetation biophysical structures. This study investigates a physically based bidirectional reflectance distribution function (BRDF) model to infer vegetation biophysical characteristics with multidirectional measurements (Fig. 3). We adapt a model by Rahman et al. (1993):

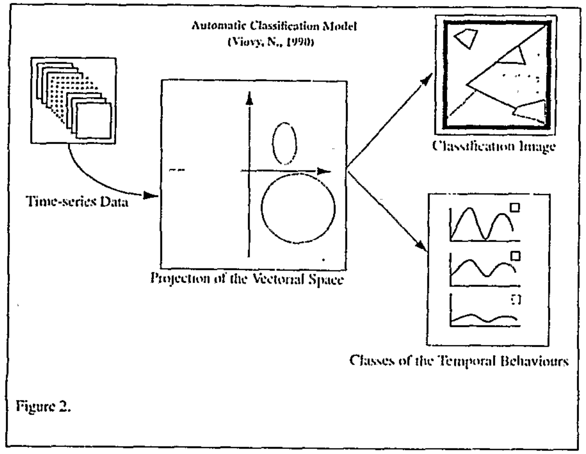

Fig. 2. Description of the automatic classification by clustering method (Viovy, 1990).

$$\rho(\Theta_s, \Theta_v, \varphi) = \rho_0 \frac{(\cos\Theta_s \cos\Theta_v)^{k-1}}{(\cos\Theta_s + \cos\Theta_v)^{1-k}} \times \frac{1-\Theta^2}{[1+\Theta^2 - 2\Theta\cos(\pi - \xi)]^{3/2}} \left(1 + \frac{1-\rho_0}{1+G}\right)$$

where G is given as

$$G = (\tan^2\Theta_s + \tan^2\Theta_v - 2\tan\Theta_s \tan\Theta_v \cos\varphi)^{1/2}$$

and ξ is given as

$$\cos\xi = \cos\Theta_s \cos\Theta_v + \sin\Theta_s \sin\Theta_v \cos\varphi$$

Variables Θ_s, Θ_v and φ are the solar zenith, viewing zenith and relative azimuth angles; ρ_0 $(0 < \rho_0 < 1)$ is related to the surface reflectances of a flat surface, mainly determined by the Lambertian part of the surface. The exponent parameter k $(0 < k < 1)$ is related to the vertical structure (non-Lambertian part), and Θ is related to the orientation of the bidirectional behaviour. Negative values of Θ refer to backscattering, and positive values refer to forward scattering. To infer vegetation properties (ρ_0, k and Θ), Rahman's model is inverted against multidirectional measurements (Qi et al., 1994).

3. Analysis and discussion

First, a map made up of 21 classes is derived by applying the automatic classification over the 2 year time-series (Fig. 4). This map delimits the drought zone in the northwest of

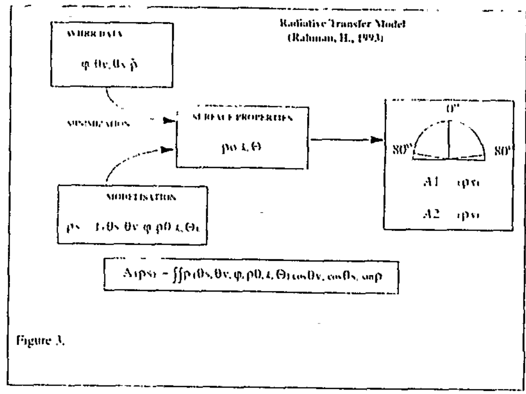

Fig. 3. Description of the radiative transfer model of Rahman et al. (1993).

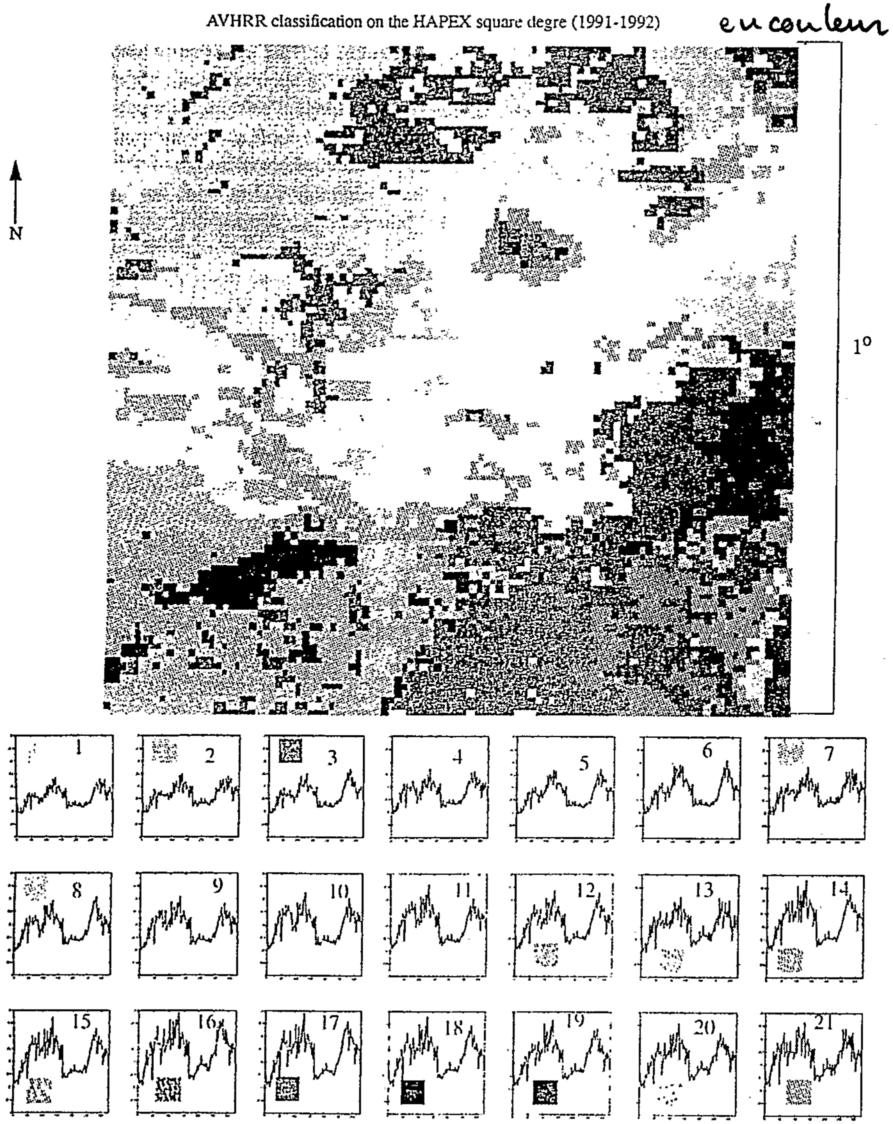

Fig. 4. AVHRR automatic classification for square degree HAPEX-Sahel experiment. The legend gives the number of classes and the corresponding colour. Each graph represents the mean class value and characterizes the rhythms and intensity of the pixel group.

the square degree (red colour groups: Class 1–7). In yellow and green (Class 8–15), different areas representative of agricultural activies can be identified. In the south of the square degree, we can note blue and violet (Class 16–21) colour groups, for which the intensity of the temporal NDVI evolution is very important. The evolution of the profiles along the north–south transect can be observed: the NDVI is higher in the south; however, the structure of the profiles seems similar. This can be explained by the fact that the temporal distribution is the same from north to south, but the amount of rain is higher

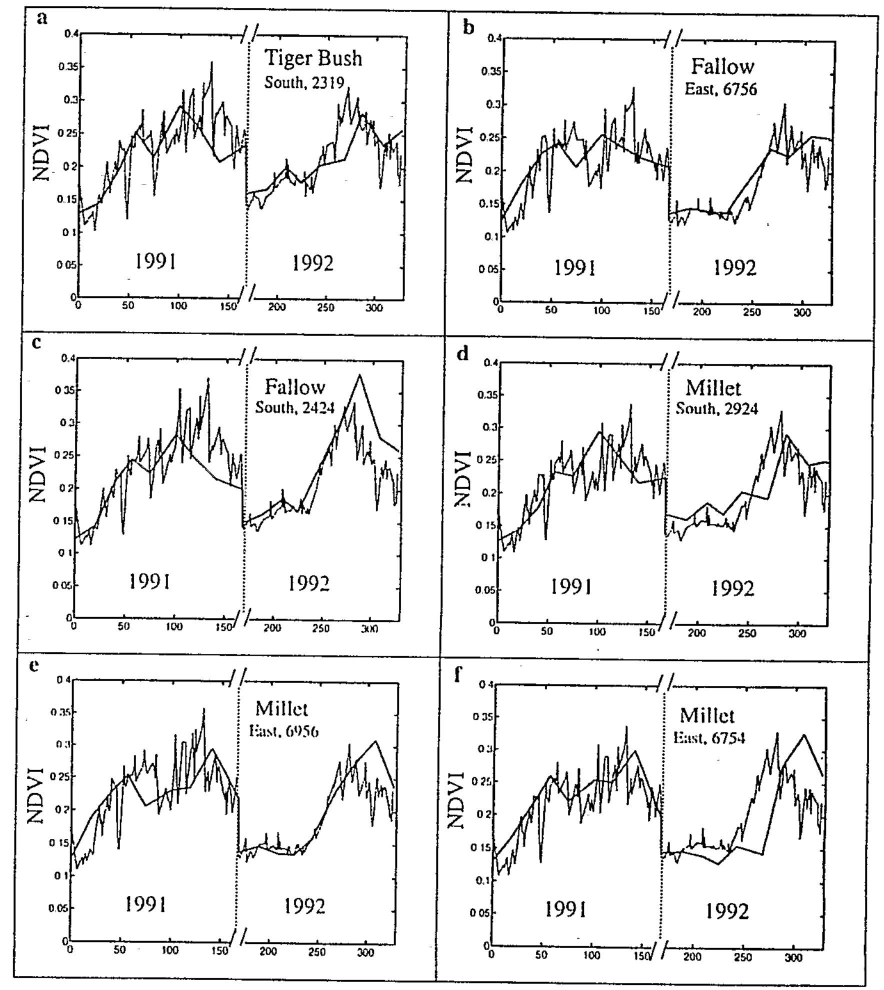

Fig. 5. Comparison between the output radiative transfer model (black curves) and the different classes obtained by the clustering method. The side-by-side subplots describe the data set for the two rainy seasons (1991 and 1992).

in the south. This is confirmed by ground measurements of rainfall and also by the ground control map (Valentin et al., 1992). It should be emphasized that the ground control map (Fig. 1) is static and has been derived using Spot data, which have a spatial resolution of 20 m, whereas the classification has been applied to time-series of AVHRR data at 1 km resolution. These differences in resolution explain why most bare soil spots, especially in the south, are clearly identified in Fig. 1 but hidden in Fig. 4. In most cases, however, the dominant vegetation is well located both in the north and in the south. These classes represent a homogeneous behaviour of the NDVI during the vegetative period. Each class seems to indicate a particular land cover or land use (see Fig. 4).

Based on the ground control map, a sample of pixels within the dominant vegetation types (i.e. millet fields, fallow and tiger bush) is selected. Then, for the whole AVHRR data set, Rahman's model is used to estimate the hemispherical albedos in the red and near-IR bands from AVHRR reflectances taken at consecutive days. The surface properties are assumed to be constant. Hemispherical albedos corresponding to nine illumination angles (from 0° to 80°) are calculated. However, only data estimated at the nadir location are used for our study. The temporal evolution of the albedo-based NDVI, corresponding to our control points of each dominant vegetation type, is computed. In Fig. 5(a)–(f), for each control point, the temporal profile of albedo-based NDVI (black line) is compared with the corresponding class profile (grey line). This figure shows that, for each selected point, the two temporal behaviours of NDVI are similar, except in 1992, when a shift between the two maxima can be detected. Different vegetation evolutions are observed for both profiles in 1991 and 1992, and can be explained by the fact that the beginning of rainfall occurred later than in 1992 in 1991. This synergy between the NDVI class and albedo-based NDVI evolutions over the three types of experiment sites suggests that the automatic classification, which is based blindly on temporal evolution agreement of the signal, seems to represent the actual evolution of the vegetation. This is a very important result, as the classification was never tested with real surface data.

4. Conclusion

Automatic classifications, in conjunction with remotely sensed data, have been widely used to characterize the spatial and temporal vegetation dynamics. In this study, a first attempt is made to investigate the significance of the results obtained by such classification in terms of physical vegetation parameters (i.e. albedo). This aim is performed by comparing, for given control points on the surface, the evolution of the albedo-based NDVI and of its corresponding class. The result shows that there is similarity between the behaviour of the 1991 and 1992 temporal profiles estimated at all control points.

Acknowledgements

This reseach has been performed with financial support of the SALT project. This study is included in the framework of the EOS hydrology project.

References

Asrar, G., Fuchs, M., Kanemasu, E.T., and Hatfield, J.L., 1984. Estimating absorbed photosynthetic radiation and leaf area index from spectral reflectance in wheat. Agron. J., 76: 300–306.

Goutorbe, J.-P., Lebel, T., Tinga, A., Bessemoulin, P., Brouwer, J., Dolman, A., Engman, E., Gash, J., Hoepffner, M., Kabat, P., Kerr, Y., Monteny, B., Prince, S., Said, F., Sellers, P. and Wallace, J., 1994. HAPEX-Sahel: a large scale study of land–atmospheric interactions in the semi-arid tropics. Ann. Geophys., 12: 53–64.

Loudjani, P., Cabot, F., Gond, V. and Viovy, N., 1994. Improving NDVI time-series using imposed threshold on Irt, Ir and Visible values (INTUITIV): a method for reducing cloud contamination and noise in NDVI time-series over tropical and sub-tropical regions. In: CNES (Editor), Proc. 6th Int. Symp. Physical Measurements and Signatures in Remote Sensing, Val d'Isère, France, pp. 93–108.

Menaut, J.-C. and Podaire, A., 1990. Projet SALT: analyse de la dynamique des changements de paysages des savanes d'Afrique de l'Ouest: mécanismes sous-jacents et spatialisation des processus. In: CNRS (Editor), Comité Ecosystèmes du Programme Français Géosphère–Biosphère. CNRS, Paris, 71 pp.

Qi, J., Huete, A., Cabot, F. and Chehbouni, A., 1994. Bidirectional properties and utilizations of high-resolution spectra from a semiarid watershed. Water Resour. Res., 30(5): 1271–1279.

Rahman, H. and Dedieu, G., 1994. SMAC: a simplified method for atmospheric correction of satellite measurements in the solar spectrum. Int. J. Remote Sens., 15: 123–143.

Rahman, H., Verstraete, M. and Pinty, B., 1993. A coupled surface–atmosphere reflectance (CSAR) model. Part 2: semi-empirical model usable with NOAA advanced very high resolution radiometer data. J. Geophys. Res., 98: 20791–20801.

Teillet, P. and Holben, B., 1994. Towards operational radiometric calibration of NOAA–AVHRR imagery in the visible and infrared channels. Can. J. Remote Sens., 20: 1-10.

Valentin, C., Courault, D., D'Herbes, J.M. and Timouk, F., 1992. Etats de surface du sol, degré², Niamey, Niger. In: ORSTOM–AGRHYMET (Editor), Niamey, Niger.

Viovy, N., 1990. Etude spatiale de la biosphère terrestre: intégration de modèles écologiques et de mesures de télédétection. Thèse de Doctorat, INPT, Toulouse, 213 pp.